Proceedings of the 3rd International Conference on Computing Innovation and Applied Physics
DOI: 10.54254/2753-8818/30/20241128

Numerical simulation of MHD on sudden expansion duct under strong transverse magnetic field

Yipeng Liu

Department of Mechanical and Aerospace Engineering, University of California Irvine, Irvine, CA 92697-4525, USA

yipengl7@uci.edu

Abstract. This research delves into the analysis of quasi-two-dimensional flow dynamics in liquid metal confined within a sudden expansion duct, subjected to a strong magnetic field. Utilizing numerical simulations derived from the SM82 model, the study concentrates on examining the magnetohydrodynamic (MHD) responses across a defined range of parameters. These simulations were conducted maintaining a constant Reynolds number (Re), while systematically varying the Hartmann number (Ha) across a spectrum of values [1000, 2000, 5000, 10000, 15000, 20000] to enable a thorough exploration of the magnetic field's influence on the flow dynamics. The outcomes of this study reveal a marked transition in flow behavior corresponding with the escalation in magnetic field strength. Notably, as the magnetic field intensifies, the flow undergoes a transformation from a state of instability to stability. This shift is predominantly characterized by a diminution, followed by a complete cessation, of shear vortex shedding. Additionally, beyond a Ha of 5000 and at a longitudinal position of x = 6, both the velocity and pressure profiles begin to exhibit near-identical and symmetric characteristics. Post the Ha exceeding 1000, the vortex profile demonstrates symmetry about the y=0 axis. These observations significantly enhance the comprehension of MHD fluid dynamics under quasi-two-dimensional conditions.

Keywords: Strong Magnetic Field, Shear Layer Shedding, quasi-two-dimensional MHD flow, flow fluctuation, Hartmann Number.

1. Introduction

In numerous engineering domains, particularly those involving intense magnetic fields such as metallurgical operations and cooling mechanisms for magnetic confinement fusion reactors, the dynamics of electrically conductive fluids in conduits have been extensively studied [1, 2]. Within the context of magnetic confinement fusion, a blanket composed of multiple channels filled with liquid metal plays a pivotal role. This blanket is instrumental in converting the energy from neutron reactions into thermal energy and facilitates the production of tritium, an essential element for nuclear fusion reactions. Among the assorted designs of liquid metal blankets, the dual-coolant lead-lithium (DCLL) blanket is distinguished by its potential for heightened thermal efficiency, superior tritium generation capabilities, and advanced safety features [3-5].

Characteristic flow patterns in DCLL blankets include a 180-degree sharp bend, poloidal parallel ducts, and sudden expansions. Recent investigations have focused on analyzing velocity distribution and

DOI: 10.54254/2753-8818/30/20241128

magnetohydrodynamic (MHD) pressure drops in the poloidal ducts of these blankets. It has been identified that the inlet and outlet manifolds primarily contribute to the MHD pressure drop within the blanket structure [4, 6]. Despite occasional consideration in the literature, the impact of sudden expansion geometries under strong magnetic fields remains insufficiently explored [7]. Comprehending the behavior of flow in the presence of sudden expansions under such magnetic conditions is crucial for accurately predicting flow dynamics within these blankets.

In the realm of magnetic confinement fusion reactors equipped with DCLL blankets, the significance of geometric considerations in the context of sudden expansions is paramount, as evidenced by references [8, 9]. The presence of a substantial magnetic field necessitates a thorough examination of the behavior of liquid metal when it moves perpendicular to this field. Such movement induces eddy currents, which, upon interacting with the magnetic field, generate an electromagnetic Lorentz force. This force inherently opposes the liquid metal's motion, as detailed in studies [10-13]. Consequently, this phenomenon has spurred extensive research into MHD flow dynamics.

A notable contribution to this field was made in 1982 by Sommeria and Moreau [13], who introduced the SM82 model. This model innovatively transformed a complex three-dimensional flow into a more manageable two-dimensional framework by averaging the flow variables along the magnetic field lines. Building upon this foundation, Zhang et al. [14] conducted a groundbreaking investigation into the flow characteristics of a metallic fluid within a vertically oriented square duct. Their research, grounded in parameters derived from actual cladding operations, marked the first exploration of flow dynamics within such a duct. They elucidated the interplay between the Reynolds number (Re), Hartmann number (Ha), and Grashoff number (Gr) in influencing the flow behavior within the duct. A key finding from their study was the identification of the stability criterion Gr=4HaRe, which offers vital insights for the design of realistic cladding systems.

Expanding upon these findings, Dousset [15] examined four distinct flow states and their corresponding parameter ranges in duct flow around a cylinder with a fixed blocking ratio, under varying conditions of Re and Ha numbers. These insights, along with discussions on various parameters affecting MHD flow, underscore the complexity and nuance of this field. However, to fully understand the Hartmann braking effects induced by strong magnetic fields, further research is essential. Such studies will be crucial in elucidating the evolution of MHD flow and its implications in practical applications.

Mistrangelo [16] investigated the flow characteristics within a duct exhibiting a sudden expansion with an Er of 4 at a low Re. The study highlighted that an increase in the magnetic field's intensity correspondingly diminished the backflow zones adjacent to the expanded duct area until their complete elimination. This investigation considered flow parameters with a Reynolds number set at Re = 100 and a Ha not exceeding 1000, parameters significantly lower than those prevalent in fusion reactors. Despite these findings, the two-dimensional turbulent flow dynamics in ducts with sudden expansions remain insufficiently explored.

The current study builds upon the SM82 model to scrutinize the impact of varying the Ha on the quasi-two-dimensional turbulent flow characteristics in the vicinity of a sudden expansion duct. This examination is conducted while maintaining constant values for other variables, such as the Re and the Er. Moreover, this research aims to contribute to the engineering field by providing generalized insights into the pressure differentials between the inlet and outlet, as well as determining friction coefficients on solid surfaces.

2. Physical Model and Problem Formulation

2.1. Physical Model

In Figure 1, the schematic representation of the geometric duct pertaining to sudden expansion is depicted. The dimension L_1 signifies the longitudinal length of the inlet duct, whereas L_e represents the length of the duct post-expansion. The width of the inlet duct is denoted by h, and the width of the expanded section is indicated by H. The ratio of the duct's length prior to and following the expansion is quantified as $L_e/L_i=4$. Furthermore, the ratio of length to width in the expanded section is expressed

DOI: 10.54254/2753-8818/30/20241128

as L_e/H=5, and the expansion ratio is defined as H/h=4. The entrance velocity at the duct's opening is designated as U. A standard depth of the duct is established, represented by z=1. The orientation of the magnetic field is aligned with the z-direction. This experimental setup is designed to investigate the impact of magnetic field strength on the shear flow induced by sudden expansion.

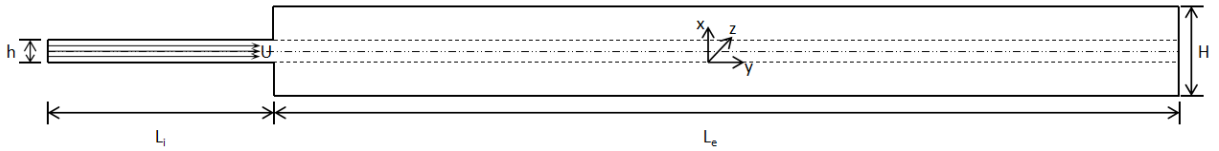

Figure 1. Schematic diagram of 2D sudden expansion duct model

2.2. Problem Formulation

In the context of this research, gravitational effects are not considered. Consequently, the duct diameter (H), peak inlet velocity (U), the dimensionless ratio H/U, and the non-dimensional parameter ρU^2 are utilized to non-dimensionalize the parameters corresponding to length, velocity, time, and pressure. Utilizing these variables, the fundamental equations governing mass and momentum are formulated as follows:

$$\nabla \cdot u = 0 \tag{1}$$

$$\frac{\partial u}{\partial t} + (u \cdot \nabla)u + \nabla p = \frac{1}{Re^2 \frac{H_d}{Re}} \tag{2}$$

In the framework, the variable u represents velocity, p denotes pressure, and t is indicative of time. The Re is defined by employing the inlet width of the sudden expansion duct, symbolized by *h*, as the reference length. Concurrently, the maximum velocity at the duct inlet is considered as the reference speed. The expression for the Re is thus established as follows:

$$\mathrm{Re} = \frac{Uh}{v} \tag{3}$$

In the context of fluid dynamics, the parameter under consideration represents the ratio of inertial forces to viscous forces, where ν symbolizes the coefficient of dynamic viscosity of the fluid. During the analytical process, the Re is quantified at a value of 50,000. According to Ha's formulation, the coefficient of friction is characterized as follows:

$$H_d = n\left(\frac{H}{a}\right)^2 Ha \tag{4}$$

The symbol 'n' is utilized to represent the aggregate count of Ha layers, aligning with the duct walls situated parallel to the x-y plane, as depicted in Figure 1 (wherein, for the purposes of these calculations, n is assigned the value of 8). Concurrently, the variable 'a' is indicative of the thickness of the duct, which is oriented in the direction of the applied magnetic field. Furthermore, the Ha, denoted as Ha, serves as a quantitative measure of the magnetic field's intensity.

$$Ha = aB\left(\frac{\sigma}{\rho v}\right)^{\frac{1}{2}} \tag{5}$$

B denotes the strength of the magnetic field, σ stands for electrical conductivity, and the interaction number is determined by the ratio of the Ha squared to the Re:

$$N = \frac{Ha^2}{Re} \tag{6}$$

describes the relationship between electromagnetic and inertial forces.

In the proposed model, which approximates a quasi-two-dimensional configuration, the dynamics of metallic fluids are forecasted in response to a substantial magnetic field. It is imperative for the precision of computational analysis that the intensity of the magnetic field is sufficiently elevated, as specified:

$$Ha >> 1, N >> 1$$

The following boundary conditions are established for numerical simulation:

$$\text{When } x = -5, u = (1,0,0), \frac{\partial p}{\partial x} = 0, \ y \in [-0.5, 0.5]$$

DOI: 10.54254/2753-8818/30/20241128

$$\text{When } x = 0, u = (0,0,0), \frac{\partial p}{\partial x} = 0, \ y \in [-2,2]$$
$$\text{When } x = 20, u = (0,0,0), \frac{\partial p}{\partial x} = 0, \ y \in [-2,2]$$
$$\text{When } y = 0.5, u = (0,0,0), \frac{\partial p}{\partial x} = 0, y = -0.5, u = (0,0,0), \frac{\partial p}{\partial x} = 0$$
$$\text{When }, y = 2, u = (0,0,0), \frac{\partial p}{\partial x} = 0, y = -2, u = (0,0,0), \frac{\partial p}{\partial x} = 0$$

3. Mesh Validation

The Hartmann layer is defined as a boundary layer that extends parallel to the conduit's wall and orthogonal to the magnetic field's orientation, occurring within a conduit subjected to a magnetic flow. This layer's thickness is related to $\delta_H \sim Ha^{-1}$. The Hartmann layer is characterized as a boundary layer that is aligned parallel to the wall of the conduit and perpendicular to the direction of the magnetic field. This layer manifests within conduits that are subject to magnetic flow, related to $\delta_H \sim Ha^{-1/2}$. In the computational analysis, the resolution of the grid in both the Hartmann and side layers emerges as a pivotal factor for ensuring the fidelity of numerical results, particularly under the influence of a strong magnetic field [17]. Within the framework of the present study, the grid resolution for the side layers has been meticulously configured to comprise eight layers. Subsequently, average values are computed along the direction of the magnetic field for models that are effectively quasi-two-dimensional. Consequently, the focus of this investigation is primarily on the grid configuration of the side layers. Existing literature [18] underscores the necessity of incorporating a minimum of eight grid points within the side layer to uphold the computational precision of the quasi-two-dimensional model. In this regard, the mean kinetic energy E of the flow field is articulated as follows:

$$E = \frac{1}{A}\int_A \left(U_x^2 + U_y^2\right) dA \tag{7}$$

In the example calculation, a comparative analysis was conducted using four distinct mesh configurations of varying dimensions. Table 1 elucidates the primary attributes, alongside the discrepancies in relative errors and kinetic energy, specifically pertaining to the primary attributes of varied mesh configurations and associated discrepancies in the friction coefficient C_f, as shown in Eq.(8), when juxtaposed against the benchmark mesh M_4 at a Re of 50,000.

$$C_f = \frac{2F_D}{\rho U_0^2 a} \tag{8}$$

The symbol X denotes the count of nodes along the x-axis in both the inlet and exit regions; Y_1 represents the node count on the y-axis within the inlet zone; Y_2 indicates the total nodes along the y-axis in the exit zone; Y_3 provides the node tally on the y-axis in the expanded segment; N_{tot} embodies the aggregate count of elements; N_{sh} signifies the quantity of elements within the Shercliff layers. And R designates the minimal resolution observed within the Shercliff layers. The findings suggest that mesh M_4 offers commendable accuracy while maintaining computational efficiency, thus proving viable for conducting parametric analyses concerning Re and Ha.

Table 1. Comparison table of correlations between four selected different meshes

Mesh	E	X	Y_1	Y_2	Y_3	N_{tot}	R	N_{Sh}	$C_f\% = \left[1 - \frac{C_f(M_i)}{C_f(M_4)}\right]$
M1	0.032%	80	200	250	80	80000	0.00252	6	0.337%
M2	0.027%	120	200	275	100	110000	0.00189	8	0.172%
M3	0.012%	160	200	300	120	150000	0.00150	10	0.0662%
M4	—	200	200	325	140	200000	0.00055	12	—

In conducting an investigation with a prescribed Re of 50,000, various mesh configurations were evaluated. The outcomes derived from the four distinct mesh groupings demonstrate a marked consistency and congruence. Notably, discrepancies in the corresponding physical measurements across these groupings are minimal, with less than 0.2% variation observed. Consequently, for the purpose of numerical analysis, the M3 configuration is identified as the most suitable selection.

DOI: 10.54254/2753-8818/30/20241128

4. Result

4.1. The effects of magnetic field on the flow state

The fluid, characterized by a reduced velocity on either side, exhibits a markedly distinct speed owing to the rapid acceleration induced by the sudden expansion. This phenomenon is further elucidated in Figure 2. As the flow progresses downstream, there is a gradual equalization and eventual stabilization of the mean flow-directional velocity across varying x-positions along the y-axis at the duct's central region, manifesting in a symmetric profile about the x=0 axis.

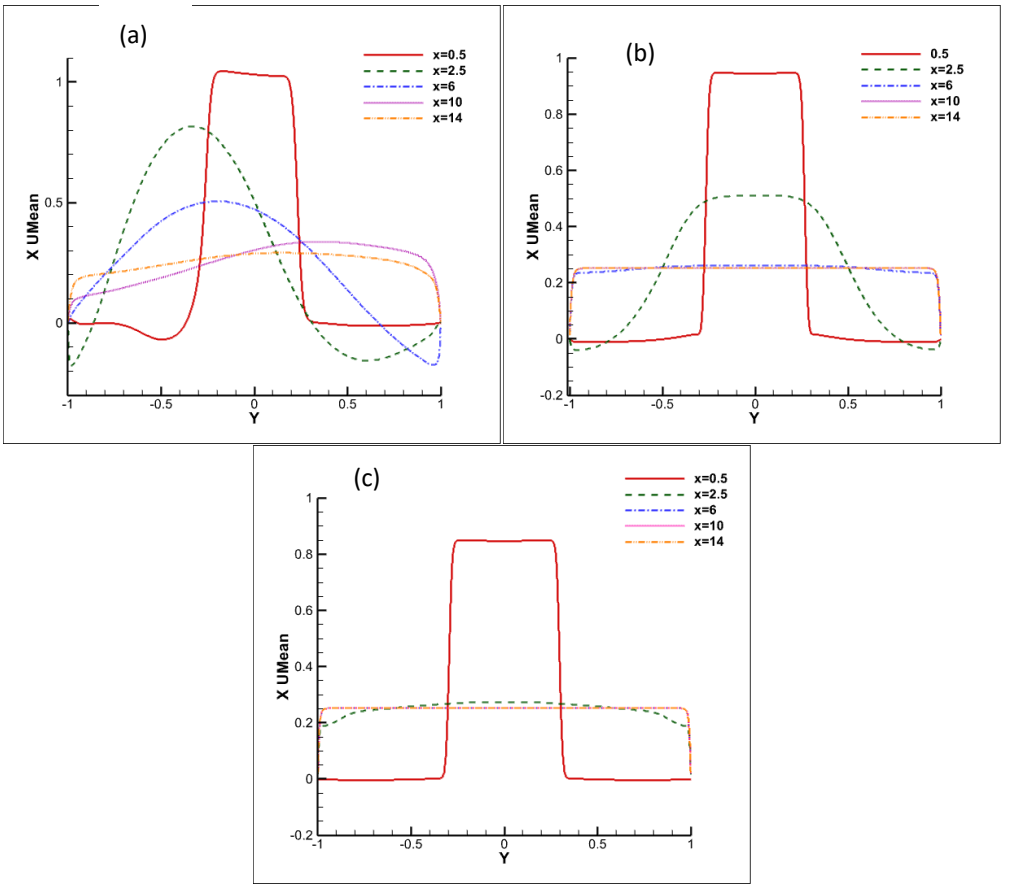

Figure 2. The mean flow-directional velocity U_x profile compared to the y-axis at different x positions when Re=50000, Ha=1000 (a), Ha=5000 (b), and Ha=10000 (c)

In the same vein, Figure 3 elucidates the variation of the duct's mean velocity in the y-direction, contingent upon its position along the y-axis at disparate x coordinates. The empirical data delineate a pattern where the velocity in the y-direction initially escalates and subsequently diminishes as the flow advances, reaching its zenith near x=2.5. Contrasting with its relatively languid movement at the peripheries of the duct, the fluid exhibits a markedly elevated velocity at the center of the jet's exit point. This differential engenders a shear layer at their confluence. Owing to this shear layer, the rapidly flowing fluid at the core begins to diverge towards the periphery, engendering a symmetric velocity profile centered at y=0. As the flow progresses downstream, the fast-moving fluid intertwines with the slower regions, resulting in a shear vortex that progressively loses stability. This shear vortex, once formed, diverges from the center due to the velocity disparity, reflecting the observed trend in Figure 3 wherein the peak U_y velocity ascends, then descends, concurrently exhibiting lateral movement. The shear vortex attenuates and the velocity discrepancy between the central and peripheral fluid diminishes

DOI: 10.54254/2753-8818/30/20241128

as the flow proceeds along the duct, mirroring the gradual reduction in U_y. Reference to the vorticity contour depicted in Figure 6(c) further substantiates these observations.

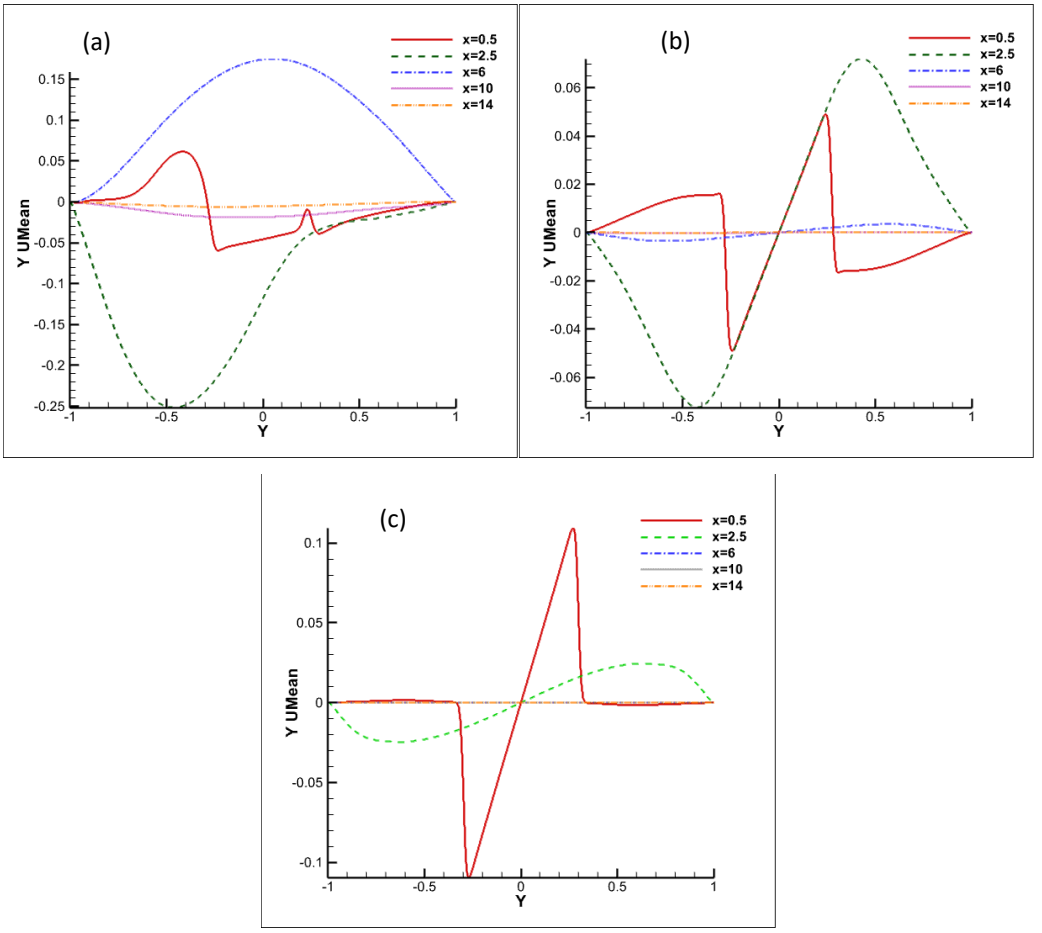

Figure 3. The mean longitudinal velocity U_y profile compared to the y-axis at different x positions when Re=50000, Ha=1000 (a), Ha=5000 (b), and Ha=10000 (c)

In Figure 4, the velocity patterns of the flow in relation to its mean velocity are depicted under varying magnetic field strengths at two distinct developmental stages: the initial phase (x=2.5) and the fully developed stage (x=10). During the early development phase, a lower Ha is associated with an expanded velocity curve, characterized by velocities approaching zero near the boundary wall. As the flow evolves, the lateral velocities converge symmetrically around y=0. Concurrently, an increase in the magnetic field strength leads to a reduction in the velocity at the duct's center. This phenomenon is further exemplified by the narrowing of the jet shear layer, as illustrated in Figure 4(a) for Ha values of 10000, 15000, and 20000. Upon reaching x=10, the flow attains a mature state, wherein the dynamics of the jet zone exert minimal influence on the velocity pattern. With the progressive augmentation of the Ha number, the velocity of the fluid flow in the duct's center tends to uniformity. In parallel, the velocity of the boundary layer exhibits a gradual increase and achieves near consistency, corroborating the findings presented in [19].

DOI: 10.54254/2753-8818/30/20241128

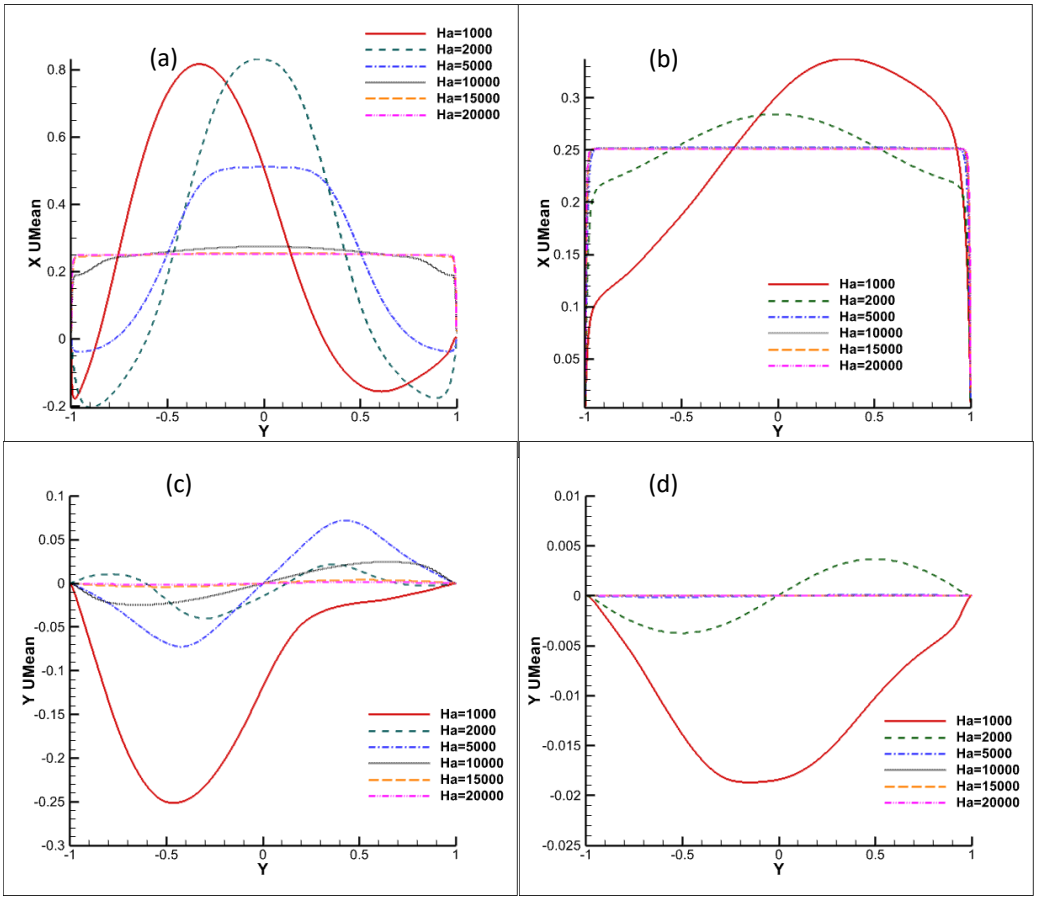

Figure 4. The mean flow direction velocity of different Ha at x=2.5 (a) and x=10 (b), and the mean longitudinal velocity of different Ha at x=2.5(c) and x=10(d)

In the context of fluid dynamics within a suddenly expanding duct under the influence of a magnetic field, two predominant flow states emerge: steady and unsteady. This dichotomy is visually represented in Figure 5, which illustrates the transient flow patterns characteristic of the unsteady state, utilizing specific parameters: Re set at 50,000 and Ha at 1,000. In this scenario, the fluid entering centrally exhibits a higher velocity, in contrast to the comparatively slower fluid influx from the lateral sides. This velocity disparity is effectively captured in the vorticity diagram of Figure 5(b), where the interaction between the differing velocity streams leads to the formation of a shear region. This region is notably characterized by a high concentration of vortices.

As the flow progresses downstream within the duct, the shear region begins to exhibit oscillatory behavior. The shedding of vortices occurs in a distinct pattern, alternating between the duct walls. These vortices progressively approach the walls, adhering to their movement. This phenomenon results in the flow intermittently separating from and reattaching to the wall surfaces. Additionally, Figure 5(a) provides a snapshot of the velocity profile in the x-direction. It distinctly shows the trajectory of a shed vortex as it reaches the rear wall at x=3, subsequently adhering to the wall, moving downstream, and eventually dissipating.

DOI: 10.54254/2753-8818/30/20241128

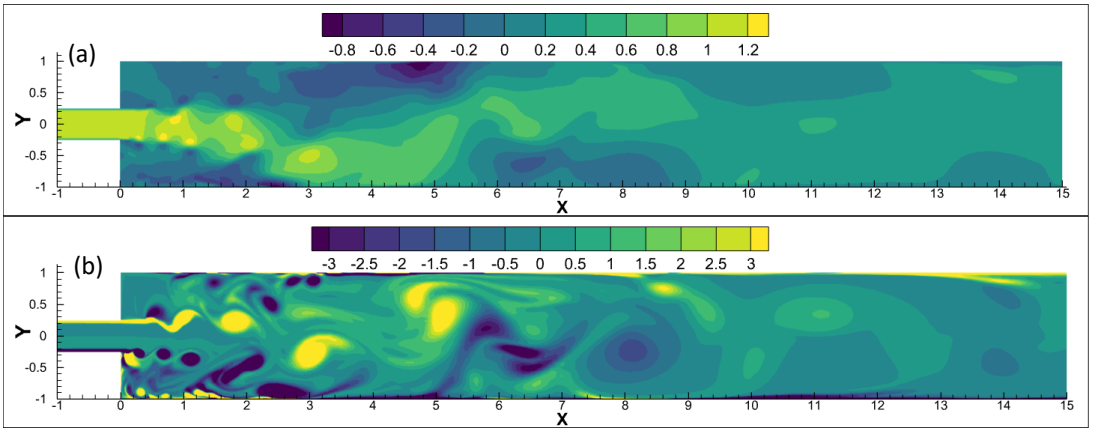

Figure 5. The flow direction mean velocity (a) and the vortex (b) at Re=50000, Ha=1000

Investigations into vortex shedding reveal a decline in layer instabilities as magnetic field strength intensifies. Figures 6(b) and 7(b) delineate the immediate flow conditions at Re of 50,000, with Ha set at 2,000 and 5,000, respectively, illustrating the vortex dynamics under these parameters. Figure 6(a) illustrates the progressive dissipation of the forming shear vortex as it advances downstream, leading to a stabilization and equilibration of flow velocity beyond the x=7 mark. Similarly, in Figure 7(a), flow velocity reaches a state of stabilization at the x=4 position.

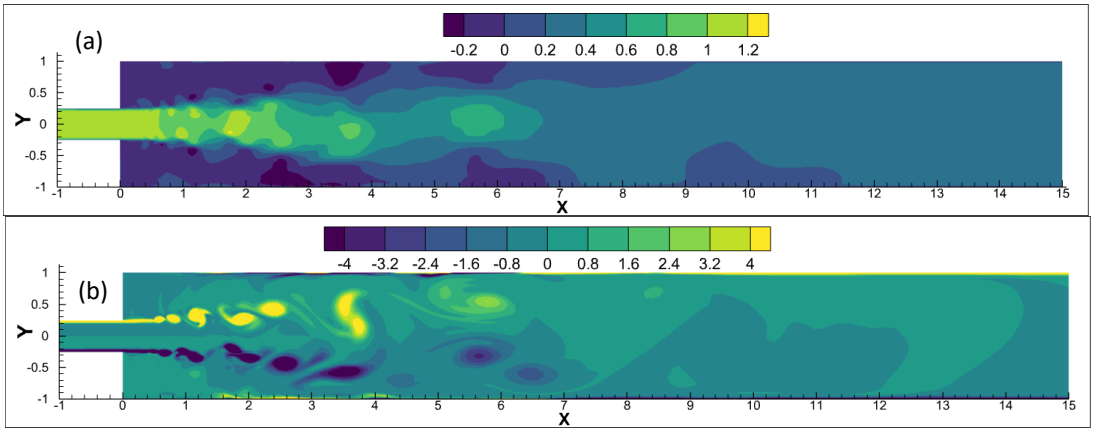

Figure 6. The flow direction mean velocity (a) and the vortex (b) at Re=50000, Ha=2000

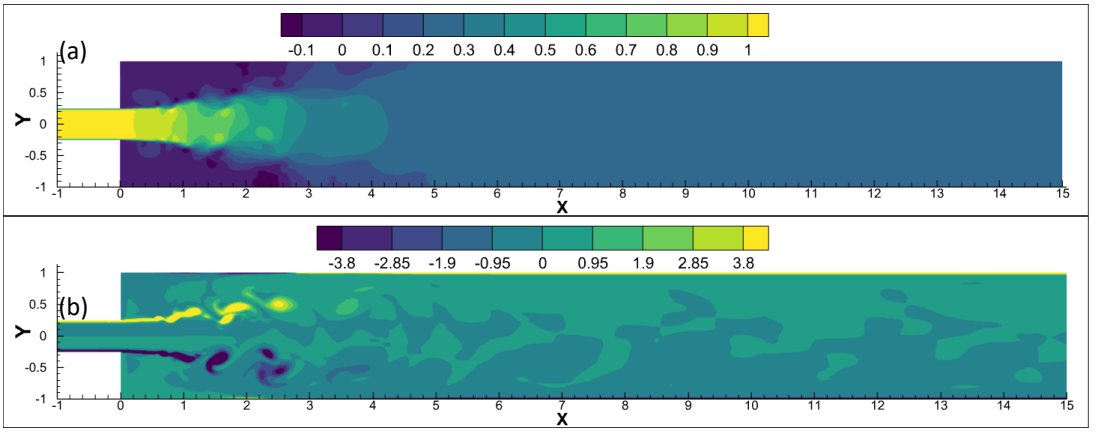

Figure 7. The flow direction mean velocity (a) and the vortex (b) at Re=50000, Ha=5000

DOI: 10.54254/2753-8818/30/20241128

In the vicinity of the walls, the flow remains stable without undergoing detachment or reattachment subsequent to the attenuation of the shear vortex. This stability is maintained without any interaction with the adjacent walls. As depicted in Figure 8, the real-time flow dynamics are illustrated under the conditions of a Re of 50,000 and a Ha of 10,000. The vorticity visualization presented in Figure 8(b) indicates that, in the presence of a strong magnetic field, the shear layer retains its stability upstream to a point of x=2. Furthermore, Figure 8(a) demonstrates that the flow velocity tends to equalize at approximately x=2, a phenomenon attributed to the influence of the magnetic field's moderation.

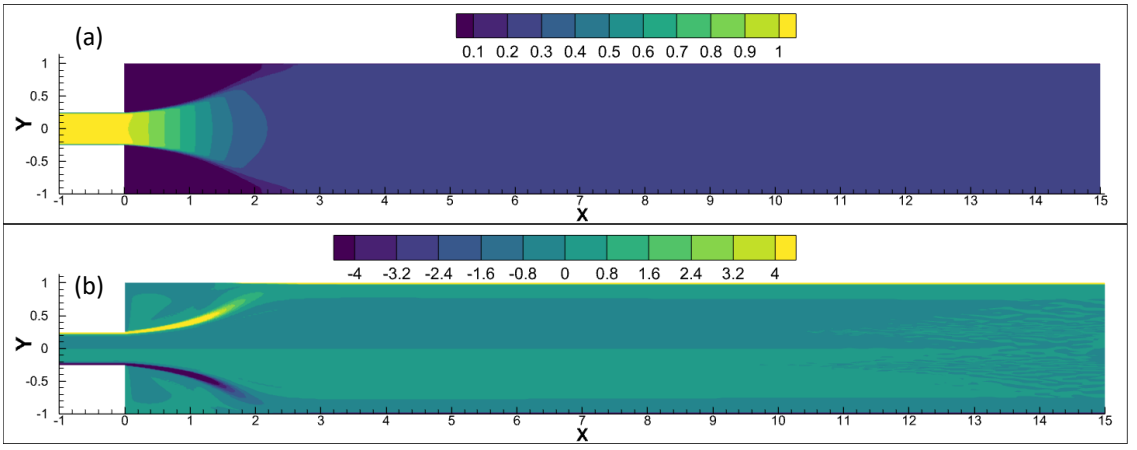

Figure 8. The flow direction mean velocity (a) and the vortex (b) at Re=50000, Ha=10000

To rigorously quantify the stable and transient characteristics of the flow domain, Figure 9 delineates the dynamic profiles of the mean kinetic energy (E) across varying Ha numbers, the mean fluctuating energy (E_{vv}) along the y-axis, and the velocity component U_x along the x-axis at a Re of 50,000. The parameter E_{vv} is defined as follows:

$$Evv = \frac{1}{A}\int_A Uy^2 dA \tag{8}$$

In the investigation, the mean kinetic energy within the flow field is explored and ascertain that the kinetic energy is significantly reduced when Ha is increased to 10,000 compared to when it is at 1,000. This observation suggests that the magnetic field plays a pivotal role in constraining the velocity of the flow. Furthermore, the study reveals that at lower Ha, the flow is subject to instability, characterized by fluctuations in its mean kinetic energy, variability in velocity, and changes in velocity along the y-axis. However, as the Ha nears 10,000, these variations tend to stabilize, leading to a negligible change in energy variation. Such stabilization is indicative of a steady state, where the velocity at each point in the flow aligns closely with the overall average velocity.

DOI: 10.54254/2753-8818/30/20241128

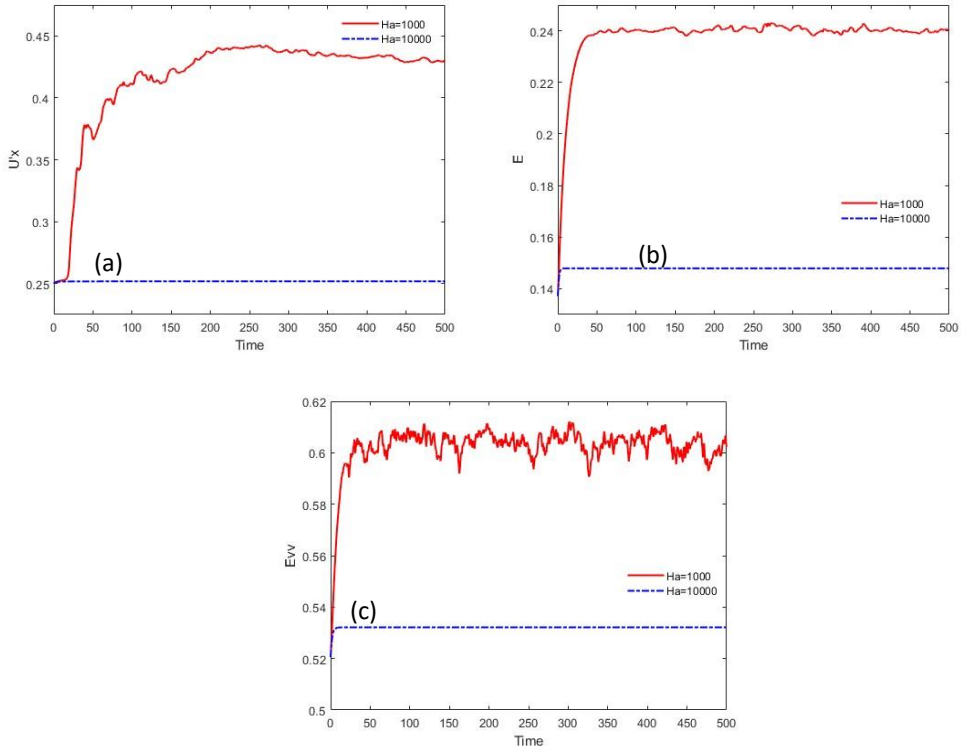

Figure 9. The probe at (6, 0.05) of the mean flow direction velocity (a), the mean kinetic energy (b), and the fluctuating kinetic energy in longitudinal direction (c)

Figure 10 illustrates the progression of average velocity in relation to the flow direction within the duct across a range of Ha. At the proximity of the jet's entry point, the flow speed remains consistent with its initial magnitude, suggesting the presence of potential flow characteristics, as referenced in [20]. The spatial extent of this region exhibits a dependency on the Ha, diminishing with an increase in Ha. Moreover, there is an exponential decline in the velocity at the central axis of the duct as the flow advances downstream.

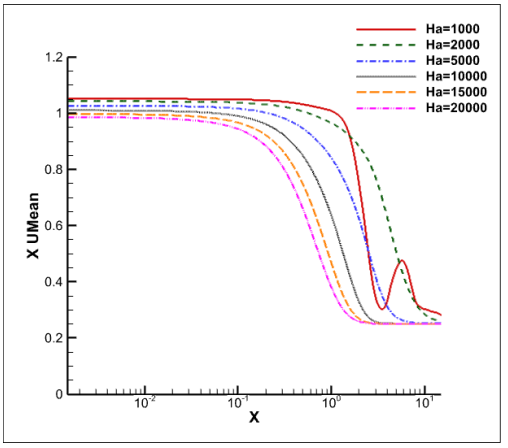

Figure 10. The mean flow direction velocity versus the x positions at the center of duct with different Ha

Figure 11 elucidates the variation of the fluctuating velocity component U_y' along the y-axis of the duct, which is aligned with the flow direction coordinate x, for various values of Ha. Notably, near the

DOI: 10.54254/2753-8818/30/20241128

duct exit, the initial magnitude of U_y' for a specific Ha is observed to be zero, denoting a state of stable flow. However, as the flow progresses downstream, there is a marked decrease in the stability of the velocity shear layer, leading to the formation of shear-induced vortices. This phenomenon causes a rapid amplification of velocity fluctuations, with a pronounced peak observed between x=3 and x=6, followed by a gradual diminution. It is also noted that the extent of stable flow from the exit point increases with an increase in Ha values. Concurrently, the peak magnitude of these fluctuations diminishes and ultimately disappears as Ha values escalate. Furthermore, the location of this peak progressively shifts downstream with higher Ha values.

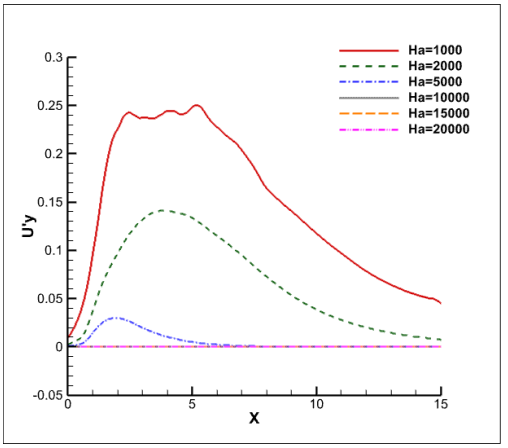

Figure 11. The fluctuating velocity of the y-direction versus x positions on the center of duct

5. Conclusion

In this research, the study builds upon the principles established in the SM82 model by Sommeria and Moreau. It utilizes the open-source computational fluid dynamics software, OpenFoam, to perform quasi-two-dimensional numerical simulations. The focus of this research is to examine the influence of strong magnetic fields on the dynamics and shear layers of a metallic fluid within a conduit, particularly in scenarios involving sudden expansion and a specific Reynolds number. This research thoroughly assesses the changes in fluid dynamics within the conduit, examining transformations in the shear layer, the development of shear vortices, and the variations in velocity distribution under different magnetic field strengths, quantified by the Ha. The results indicate that with increasing magnetic field strength, the fluid behavior within the conduit shifts from chaotic to more uniform patterns. Additionally, intense magnetic fields significantly inhibit the formation and movement of shear vortices. The mean velocity in the central fluid path demonstrates a power-law decay in the primary flow region. Furthermore, higher magnetic field intensities correlate with a reduced longitudinal extent of the shear layer, while its transverse aspect ratio increases. There is also a notable synchronization and reflection of inherent frequencies within the shear layer under these conditions.

References

[1] Abdou M., Morley N., Ying A., Smolentsev S. and Calderoni P. 2005 Overview of fusion blanket R & D in the US over the last decade Nucl. Eng. Technol. 37 401

[2] Kumar, E. R., Danani, C., Sandeep, I., Chakrapani, Ch., Pragash, N. R., Chaudhari, V., Rotti, C., Raole, P. M., Alphonsa, J., Deshpande, S. P. (2008). Preliminary design of Indian test blanket module for ITER. Fusion Engineering and Design, 83(7–9), 1169–1172.

[3] Malang, S., Tillack, M., Wong, C. P., Morley, N., Smolentsev, S. (2011). Development of the lead lithium (DCLL) blanket concept. Fusion Science and Technology, 60(1), 249–256.

[4] Smolentsev, S., Moreau, R., Bühler, L., Mistrangelo, C. (2010). MHD thermofluid issues of liquid-metal blankets: Phenomena and advances. Fusion Engineering and Design, 85(7–9), 1196–1205.

DOI: 10.54254/2753-8818/30/20241128

[5] Smolentsev, S., Morley, N. B., Abdou, M. A., Malang, S. (2015). Dual-coolant lead–lithium (DCLL) blanket status and R&D needs. Fusion Engineering and Design, 100, 44–54.
[6] Mistrangelo, C., Bühler, L. (2014). Liquid metal magnetohydrodynamic flows in manifolds of dual coolant lead lithium blankets. Fusion Engineering and Design, 89(7–8), 1319–1323.
[7] Mistrangelo, Chiara. (2006). Three-dimensional MHD flow in sudden expansions. Forschungszentrum Karlsruhe.
[8] Barleon, L., Casal, V., Lenhart, L. (2003). MHD flow in liquid-metal-cooled blankets. Fusion Engineering and Design, 14(3–4), 401–412.
[9] Chen, L., Smolentsev, S., Ni, M.-J. (2020). Toward full simulations for a liquid metal blanket: MHD flow computations for a PbLi blanket prototype at ha 104. Nuclear Fusion, 60(7), 076003.
[10] Pothérat, A. (2007). Quasi-two-dimensional perturbations in duct flows under transverse magnetic field. Physics of Fluids, 19(7).
[11] Pothérat, A.., Sommeria, J., Moreau, R. (2000). An effective two-dimensional model for MHD flows with transverse magnetic field. Journal of Fluid Mechanics, 424, 75–100.
[12] Pothérat, A.., Sommeria, J., Moreau, R. (2005). Numerical simulations of an effective two-dimensional model for flows with a transverse magnetic field. Journal of Fluid Mechanics, 534, 115–143.
[13] Sommeria, J. Moreau, R. (1982). Why, how, and when, MHD turbulence becomes two-dimensional. Journal of Fluid Mechanics, 118(1), 507.
[14] Zhang, X., Zikanov, O. (2018). Convection instability in a downward flow in a vertical duct with strong transverse magnetic field. Physics of Fluids, 30(11).
[15] Dousset, V., Pothérat, A. (2008). Numerical simulations of a cylinder wake under a strong axial magnetic field. Physics of Fluids, 20(1).
[16] Mistrangelo, C. (2011). Topological analysis of separation phenomena in liquid metal flow in sudden expansions. part 2. magnetohydrodynamic flow. Journal of Fluid Mechanics, 674, 132–162.
[17] Hussam W K, Sheard G J. Heat Transfer in a High Hartmann Number MHD Duct Flow With a Circular Cylinder Placed Near the Heated Side-wall [J]. International Journal of Heat and Mass Transfer, 2013, 67: 944–954
[18] Chatterjee D, Gupta S K. MHD Flow and Heat Transfer behind a Square Cylinder in a Duct under Strong Axial Magnetic Field [J]. International Journal of Heat and Mass Transfer, 2015, 88: 1-13
[19] Hussam, W. K., Thompson, M. C., Sheard, G. J. (2011). Dynamics and heat transfer in a quasi-two-dimensional MHD flow past a circular cylinder in a duct at High Hartmann number. International Journal of Heat and Mass Transfer, 54(5–6), 1091–1100.
[20] Deo, R. C., Mi, J., Nathan, G. J. (2008). The influence of Reynolds number on a plane jet. Physics of Fluids, 20(7).